

Breakdown of heavy quasiparticles in a honeycomb Kondo lattice: A quantum Monte Carlo study

Marcin Raczkowski,¹ Bimla Danu,¹ and Fakher F. Assaad²

¹*Institut für Theoretische Physik und Astrophysik,
Universität Würzburg, 97074 Würzburg, Germany*

²*Institut für Theoretische Physik und Astrophysik and Würzburg-Dresden Cluster of Excellence ct.qmat,
Universität Würzburg, 97074 Würzburg, Germany*
(Dated: September 16, 2022)

We show that for the half-filled Kondo lattice model on the honeycomb lattice a Kondo breakdown occurs at small Kondo couplings J_k within the magnetically ordered phase. Our conclusions are based on auxiliary field quantum Monte Carlo simulations of the so-called composite fermion spectral function. Within a U(1) gauge theory formulation of the Kondo model, it becomes apparent that a Higgs mechanism dictates the weight of the resonance in the spectral function. For the honeycomb lattice we observe that for small J_k the quasiparticle pole gives way to incoherent spectral weight but it remains well defined for the square lattice. Our result provides an explicit example where the magnetic transition and the breakdown of heavy quasiparticles are detached as observed in Yb(Rh_{0.93}Co_{0.07})₂Si₂ [Friedemann et al., Nat. Phys. **5**, 465 (2009)].

Strongly correlated many body systems are characterized by the emergence of new elementary excitations. This can occur through the fractionalization of the electron within a parton type construction – fractional quantum Hall effect [1] or Luttinger liquids [2] – or through the formation of a composite object. Examples of the latter range from the understanding of single-hole dynamics in quantum antiferromagnets [3, 4] to the emergence of the electron in \mathbb{Z}_2 lattice gauge theories in which the electron is a bound state of an orthogonal fermion and \mathbb{Z}_2 matter [5–7].

The Kondo effect is yet another example of the emergence of a composite fermion carrying the quantum numbers of the electron. Consider a spin-1/2 magnetic impurity embedded in Fermi liquid with finite density of states at the Fermi energy. In the presence of time reversal symmetry the Kondo coupling between the impurity and Fermi liquid is always relevant and leads to the emergence of a composite fermion. It consists of the spin-1/2 and conduction electrons and becomes itinerant thereby releasing the $\ln(2)$ entropy. If one replaces the metal by a Dirac liquid with vanishing density of states at the Fermi energy, the Kondo coupling is irrelevant and one will generically observe a transition from an unscreened to screened moment at finite value of the Kondo coupling [9, 10]. This transition corresponds to the breakdown of the aforementioned composite fermion [11, 12]. Such phenomena are not limited to the realm of impurity physics [13]. Neutron scattering experiments of metallic Yb₂Pt₂Pb [14] suggest a Kondo breakdown phase of a one-dimensional spin chain embedded in a three-dimensional metal. Furthermore, numerical evidence of this state of matter has been observed in models of spin chains on semimetals [15]. In dense systems such as in YbRh₂Si₂ [16–18] or CeCoIn₅ [19], the notion of Kondo breakdown or orbital Mott selective transitions [20] has deep implications since the composite fermions drop out

from the Luttinger count. For systems with an *odd* number of localized spins per unit cell and no further spontaneous symmetry breaking, this implies a violation of the Luttinger sum rule. Owing to Oshikawa’s [21] work such a violation can be understood if the spin system shows topological degeneracy akin of a spin liquid [22, 23]. For an *even* number of spins per unit cell, such topological constraints do not hold. In this case, Kondo breakdown

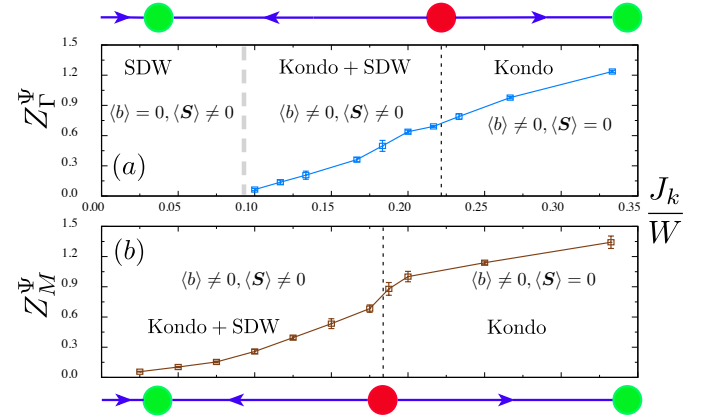


FIG. 1. Ground-state phase diagram of the half-filled Kondo lattice model on the honeycomb and square lattices. On both lattices we observe a magnetic order-disorder transition denoted by a red circle and order parameter corresponding to $\langle S \rangle$. For the honeycomb lattice (a) we observe a breakdown of the heavy quasiparticle in the spin-density-wave (SDW) phase as indicated by the vanishing residue $Z_{\mathbf{k}}^{\psi}$ of the pole at the Γ point in the composite fermion Green’s function. For the square lattice (b) we observe only the order-disorder transition since, down to our lowest value $J_k/W = 0.025$, $Z_{\mathbf{k}}^{\psi}$ at the $M = (\pi, \pi)$ point remains finite. All the values of $Z_{\mathbf{k}}^{\psi}$ are extrapolated to the thermodynamic limit [8]. We use the mean-field notation, $\langle b \rangle$, to track the magnitude of the residue.

does not imply a violation of Luttinger's theorem.

Since the tight binding model on the honeycomb lattice provides a realization of Dirac electrons, one may ask the question if and how the aforementioned Kondo breakdown transition in the impurity limit [9, 10] is carried over to the dense case described by the half-filled Kondo lattice model. In Ref. [24] it is argued that the Kondo coupling is marginal in the weak coupling limit thereby opening the possibility of Kondo breakdown transitions in magnetically ordered metallic states. The central result of this Letter is summarized in Fig. 1: Kondo breakdown indeed occurs within the magnetic phase of the honeycomb lattice. In contrast no breakdown is observed on the square lattice.

U(1) gauge theory approach. Since the Kondo effect and concomitant emergence of the composite fermion is not related to spontaneous symmetry breaking, some care has to be taken in defining the onset of these phenomena. They become particularly transparent within a U(1) gauge theory approach to the Kondo lattice model [25–27]. The Kondo lattice model (KLM) on the honeycomb lattice reads:

$$\hat{H}_{KLM} = \sum_{i,j} T_{i,j} \hat{c}_i^\dagger \hat{c}_j + \frac{J_k}{2} \sum_i \hat{c}_i^\dagger \boldsymbol{\sigma} \hat{c}_i \cdot \hat{\mathbf{S}}_i, \quad (1)$$

$$S = S_0^c + \int_0^\beta d\tau \left\{ \sum_i \left[\frac{2}{J_k} |b_i(\tau)|^2 + ia_{0,i}(\tau) + \mathbf{f}_i^\dagger(\tau) [\partial_\tau - ia_{0,i}(\tau)] \mathbf{f}_i(\tau) + b_i(\tau) \mathbf{c}_i^\dagger \mathbf{f}_i + \overline{b_i(\tau)} \mathbf{f}_i^\dagger \mathbf{c}_i \right] \right\} \quad (2)$$

with $S_0^c = \int_0^\beta d\tau \sum_{i,j} \mathbf{c}_i^\dagger(\tau) [\partial_\tau \delta_{i,j} + T_{i,j}] \mathbf{c}_j(\tau)$. The above corresponds to the action in the limit $U \rightarrow \infty$ where local U(1) gauge invariance is apparent. In particular the canonical transformation, $\mathbf{f}_i(\tau) \rightarrow \tilde{\mathbf{f}}_i(\tau) e^{i\chi_i(\tau)}$ amounts to redefining the fields $a_{0,i}(\tau) \rightarrow a_{0,i}(\tau) + \partial_\tau \chi_i(\tau)$ and $b_i(\tau) \rightarrow b_i(\tau) e^{-i\chi_i(\tau)}$, such that the partition function remains invariant. We are now in a position to probe for various phases with gauge invariant quantities. Magnetism, triggered by the RKKY interaction, corresponds to a spontaneous global SU(2) spin symmetry breaking and long ranged correlations of the order parameter $\hat{\mathbf{S}}_i = \frac{1}{2} \hat{\mathbf{f}}_i^\dagger \boldsymbol{\sigma} \hat{\mathbf{f}}_i$. Clearly $\hat{\mathbf{S}}_i$ carries no U(1) charge. To define the Kondo effect we consider the fermion field

$$\tilde{\mathbf{f}}_i(\tau) = e^{i\varphi_i(\tau)} \mathbf{f}_i(\tau), \text{ with } e^{i\varphi_i(\tau)} = \frac{b_i(\tau)}{|b_i(\tau)|}. \quad (3)$$

As argued in the Supplemental Material [8], $\tilde{\mathbf{f}}_i(\tau)$ has the quantum numbers of a physical fermion: it carries no gauge charge, has an electron charge e , and spin 1/2. The Kondo effect corresponds to the emergence of this fermion at low energies as signaled by a pole (resonance) in the dense case (single impurity limit) in the corresponding spectral function [28, 29]. There is no sym-

metry that imposes $\langle \tilde{\mathbf{f}}_i(\tau) \tilde{\mathbf{f}}_j^\dagger(\tau') \rangle$ to vanish between two space-time points and the pole in the corresponding spectral function reflects this fact. Furthermore, if the ground state turns out to be a Fermi liquid, the Luttinger volume will have to account for the composite fermion.

The above can be understood in terms of a Higgs [30] mechanism in which the phase fluctuations of $\varphi_i(\tau)$ become very slow such that $\varphi_i(\tau)$ can be set to a constant. In this case there is no distinction between $\tilde{\mathbf{f}}_i(\tau)$ and $\mathbf{f}_i(\tau)$ or, in other words, $\mathbf{f}_i(\tau)$ has lost its gauge charge and has acquired a unit electric charge. This Higgs mechanism is captured in mean-field large- N approaches of the Kondo lattice where Kondo screening corresponds to $\langle b_i(\tau) \rangle \neq 0$ [31, 32].

The above definition of the fermion field, $\tilde{\mathbf{f}}$, depends explicitly on the gauge field that is not accessible in generic numerical simulations (e.g. exact diagonalization). However, reintroducing amplitude fluctuations of the b -field, we have $\tilde{\mathbf{f}}_i \propto b_i(\tau) \mathbf{f}_i(\tau) \propto [\mathbf{f}_i^\dagger(\tau) \mathbf{c}_i(\tau)] \mathbf{f}_i(\tau)$. As shown in Ref. [33] and in the large- N limit, the right hand side of the latter equation is nothing but the composite fermion field:

$$\tilde{\mathbf{f}}_i \propto \psi_i = \mathbf{S}_i \cdot \boldsymbol{\sigma} \mathbf{c}_i. \quad (4)$$

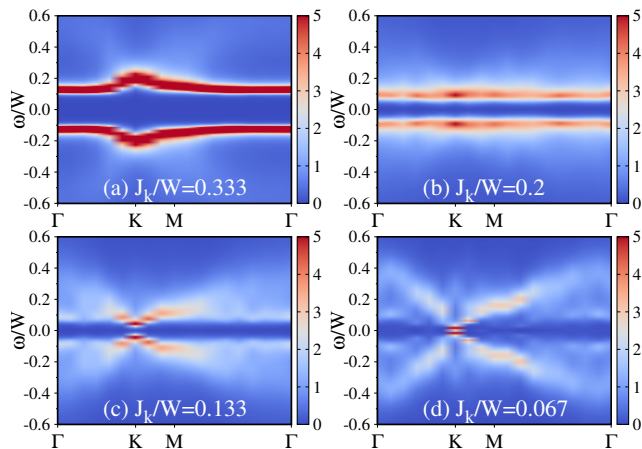


FIG. 2. Composite fermion spectral function $A_\psi(\mathbf{k}, \omega)$ along the Γ - K - M - Γ path in momentum space with $\Gamma = (0, 0)$, $K = (\frac{4\pi}{3}, 0)$, and $M = (\pi, \frac{\pi}{\sqrt{3}})$ on the $L = 18$ honeycomb KLM for representative values of J_k/W corresponding to: (a) Kondo; (b) and (c) Kondo+SDW, and (d) SDW phases.

We also note that $\langle b_i b_i^\dagger \rangle \propto \langle \hat{V}_i^\dagger \hat{V}_i \rangle \propto \langle \hat{\mathbf{c}}_i^\dagger \boldsymbol{\sigma} \hat{\mathbf{c}}_i \cdot \hat{\mathbf{S}}_i \rangle$ such that the local spin correlations between the conduction electrons and impurity spins correspond to the modulus of the boson field. If this quantity remains finite in the considered parameter regime, we will conclude that an adequate gauge field independent representation of $\hat{\mathbf{f}}_i$ is given by the composite fermion field ψ_i [34, 35]. For impurity problems the Green's function of $\hat{\psi}_i^\dagger$ corresponds to the T -matrix [36] while $\hat{\psi}_i^\dagger$ itself corresponds to the Schrieffer-Wolff transformation of the localized electron operator in the realm of the Anderson model [28].

Method. For our simulations we use the projective (zero-temperature) version of the Algorithms for Lattice Fermions (ALF) [37] implementation of the auxiliary field quantum Monte Carlo (QMC) method [38–42]. For a proper comparison between honeycomb and square lattices, we set hereafter their respective tight binding bandwidths $W = 6t$ and $W = 8t$ as the energy units.

Results. We first focus on the quantum phase transition between the magnetically ordered and disordered (Kondo) insulators and locate the phase boundary by carrying out a finite-size scaling analysis. As detailed in Ref. [8], the best data collapse gives the critical value $J_k^c/W = 0.2227(3)$ and confirms the expected universality class of the three-dimensional classical Heisenberg (O(3)) model.

Next, we turn to the evolution of the momentum resolved spectral function of the composite fermion $A_\psi(\mathbf{k}, \omega) = -\frac{1}{\pi} \text{Im} G_\psi^{\text{ret}}(\mathbf{k}, \omega)$ with $G_\psi^{\text{ret}}(\mathbf{k}, \omega) = -i \int_0^\infty dt e^{i\omega t} \sum_\sigma \langle \{ \hat{\psi}_{\mathbf{k}, \sigma}(t), \hat{\psi}_{\mathbf{k}, \sigma}^\dagger(0) \} \rangle$. In Fig. 2(a) with $J_k/W = 0.333$ deep in the Kondo phase, the emergent composite fermions are clearly manifest as bright weakly dispersive bands throughout the whole irreducible Brillouin zone. These bands become less pronounced

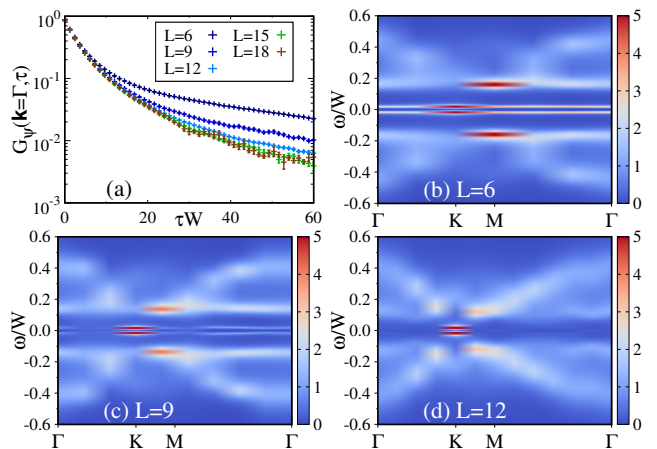


FIG. 3. (a) Composite fermion Green's function $G_\psi(\mathbf{k} = \Gamma, \tau)$ at $J_k/W = 0.067$, and (b)-(d) the corresponding spectral function $A_\psi(\mathbf{k}, \omega)$ on the honeycomb KLM with different sizes L .

upon crossing over to the magnetically ordered phase, see Figs. 2(b) and 2(c), while some incoherent spectral weight sets in at high energies. In contrast, the spectrum in Fig. 2(d) with $J_k/W = 0.067$ deep inside the magnetic phase, looks different: the composite fermion bands have disappeared indicative of the breakdown of Kondo screening. If Kondo screening is not present in the magnetically ordered phase, one can adopt a large- S approximation. In leading order in S , the spectral function $A_\psi(\mathbf{k}, \omega)$ will follow the conduction electron spectral function $A_c(\mathbf{k}, \omega)$, i.e., $A_\psi(\mathbf{k}, \omega) \simeq S^2 A_c(\mathbf{k}, \omega)$ [33]. A comparison of $A_\psi(\mathbf{k}, \omega)$ in Fig. 2(d) with the corresponding spectrum $A_c(\mathbf{k}, \omega)$ included in Ref. [8], confirms this expectation and allows one to recognize in $A_\psi(\mathbf{k}, \omega)$ a pronounced image of the conduction electron band consistent with the large- S limit.

In order to get further insight into the observed rearrangement of spectral weight in $A_\psi(\mathbf{k}, \omega)$, we plot in Fig. 3(a) raw data of $G_\psi(\mathbf{k}, \tau)$ at the Γ point at our smallest Kondo coupling $J_k/W = 0.067$ for different system sizes L . Generically, the existence of long lived quasiparticles requires that the Green's function displays a free particle behavior at long imaginary times, $G(\mathbf{k}, \tau) \xrightarrow{\tau \rightarrow \infty} Z_{\mathbf{k}} e^{-\Delta_{qp}(\mathbf{k})\tau}$, where $Z_{\mathbf{k}}$ is the quasiparticle residue of the doped hole at momentum \mathbf{k} and frequency $\omega = -\Delta_{qp}$. As is apparent, the $L = 6$ data quickly converge to the exponential decay, which as shown in 3(b), deceptively generates a low energy pole, and consequently a well defined composite fermion band, in the corresponding spectral function $A_\psi(\mathbf{k}, \omega)$. On the other hand, upon increasing system size it becomes more difficult to track the exponential form of $G_\psi(\mathbf{k} = \Gamma, \tau)$ whose long time tail systematically flattens. As a consequence, while a faint signature of the composite fermion band can still be spotted in $A_\psi(\mathbf{k}, \omega)$ for $L = 9$, see Fig. 3(c), the band has essentially disappeared from the $L = 12$

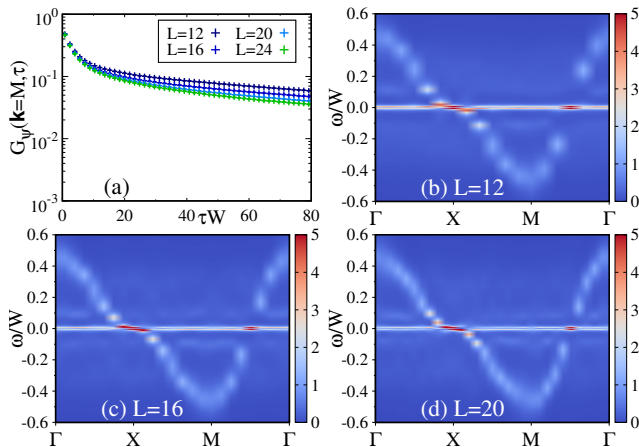


FIG. 4. (a) Composite fermion Green's function $G_\psi(\mathbf{k} = M, \tau)$, where $M = (\pi, \pi)$, at $J_k/W = 0.025$, and (b)-(d) the corresponding spectral function $A_\psi(\mathbf{k}, \omega)$ along the Γ - X - M - Γ path, where $X = (\pi, 0)$, on the square KLM with different sizes L .

spectrum in Fig. 3(d). At the same time, the overall spectrum around the Γ point broadens substantially and may plausibly be thought of as a continuum that stems from decay of the composite quasiparticle. Thus, the data are suggestive of the absence of Kondo screening in the thermodynamic limit.

It is striking to compare the results in Fig. 3 with those on the square lattice obtained at even smaller value of $J_k/W = 0.025$, see Fig. 4. Irrespective of the system size L , the composite fermion Green's function $G_\psi(\mathbf{k}, \tau)$ at the $M = (\pi, \pi)$ point shows the same asymptotic behavior in the long time limit which implies the continued existence of the pole in the corresponding spectrum $A_\psi(\mathbf{k}, \omega)$, see Figs. 4(b)-4(d). As can be seen, $A_\psi(\mathbf{k}, \omega)$ shares aspects of both the large- N approach (flat composite fermion bands) and large- S limit, i.e., the image of the conduction electron band shifted by the antiferromagnetic wavevector $\mathbf{Q} = (\pi, \pi)$. Taken together, these spectral features imply coexistence of coherent Kondo screening and long range magnetic order.

To substantiate the vanishing of the composite fermion band as a function of J_k/W , we extract the quasiparticle residue $Z_{\mathbf{k}}^\psi$ at the Γ point by fitting the long time tail of $G_\psi(\mathbf{k} = \Gamma, \tau)$ to the exponential form followed by the finite-size scaling analysis [8]. For comparison, we have equally analyzed the asymptotic behavior of $G_\psi(\mathbf{k}, \tau)$ at the M point on the square lattice and constructed the respective phase diagrams compiled in Fig. 1.

Since increasing J_k promotes the Kondo effect, it ultimately drives the magnetic order-disorder transition that occurs at $J_k^c/W \simeq 0.223$ (honeycomb) and $J_k^c/W \simeq 0.181$ (square) [43–45]. Thus, the strong coupling region in Fig. 1 is lattice independent and hosts a Kondo screened phase. In contrast, a weak coupling part of the phase diagram turns out to be non-generic: While pinning down

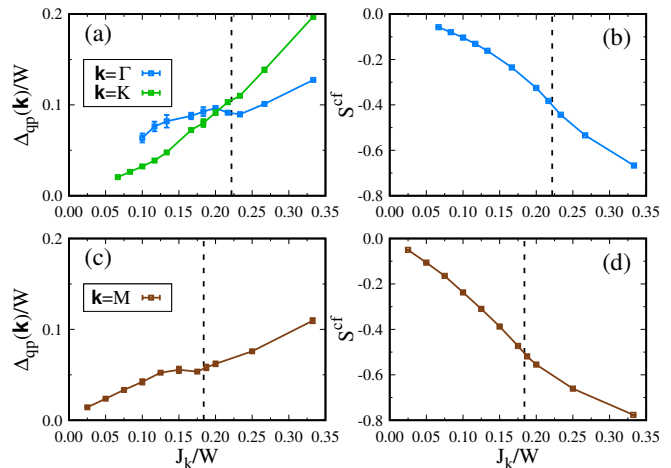


FIG. 5. (a) Single particle gap $\Delta_{qp}(\mathbf{k})$ at the Γ and Dirac K points and (b) the local spin-spin correlation function $S^{cf} = \frac{2}{3N} \sum_i \langle \hat{c}_i^\dagger \boldsymbol{\sigma} \hat{c}_i \cdot \hat{\mathbf{S}}_i \rangle$ as a function of J_k/W on the honeycomb lattice. For comparison, we show in (c) $\Delta_{qp}(\mathbf{k})$ at the M point and (d) S^{cf} on the square lattice. Dashed lines denote the respective magnetic order-disorder transitions. All quantities are representative of the thermodynamic limit [8].

the precise scaling of $Z_{\mathbf{k}}^\psi$ at the Γ point on the honeycomb lattice is a challenge, our data show that it is a monotonically decreasing function of J_k/W and vanishes slightly below $J_k/W = 0.1$. The vanishing quasiparticle residue indicates that composite quasiparticles lose their integrity. We interpret this as the destruction of Kondo screening. This is in stark contrast to the square lattice where composite fermions are found down to our smallest value $J_k/W = 0.025$ as signaled by a finite quasiparticle residue $Z_{\mathbf{k}}^\psi$ at the M point.

We also track the location and the size of the quasiparticle gap. Given that at large J_k/W the quasiparticle gap is located at the Γ point while the noninteracting model features gapless Dirac excitations at the K point, one shall resolve a change in the position of the minimal gap as a function of J_k/W . The data in Fig. 5(a) extracted from the long time behavior of $G_\psi(\mathbf{k}, \tau)$ at the both \mathbf{k} points confirm this expectation. As is apparent, the change takes place on the magnetically ordered side of J_k^c but far away from Kondo breakdown. Further, the comparison of Figs. 5(a) and 5(c), the latter showing the evolution of the quasiparticle gap at the M point on the square lattice, reveals two common features: (i) the development of the cusp preceding the magnetic order-disorder transition, and (ii) a linear in J_k/W scaling of the gap in the weak coupling limit. It is a direct consequence of the Fermi surface nesting-driven magnetic order and can be captured within a mean-field SDW framework [46, 47].

Finally, as shown in Fig. 5(b) we do not resolve any signs of the breakdown of Kondo screening in the local spin-spin correlation function $S^{cf} = \frac{2}{3N} \sum_i \langle \hat{c}_i^\dagger \boldsymbol{\sigma} \hat{c}_i \cdot$

\hat{S}_i) which remains finite down to our lowest value of J_k/W , just like that measured on the square lattice, see Fig. 5(d). This seemingly counterintuitive result becomes clear by noting that S^{cf} measures the amplitude of the boson field, $|b|^2$. Hence, Fig. 5(b) implies that the modulus of the boson field remains constant for all values of the Kondo coupling and that Kondo breakdown occurs due to phase fluctuations. The latter explains the failure of the mean-field approaches to provide consistent results for both lattices [8].

Summary and conclusions. We have investigated a Kondo breakdown defined by the *destruction* of the composite fermion in Eq. (3). In the realm of the Kondo lattice considered here, this amounts to the loss of a pole in the composite fermion Green's function. Our main result, is that Kondo breakdown occurs in the magnetic phase of the half-filled KLM on the honeycomb lattice. This stands in stark contrast to our results on the square lattice where down to the lowest values of the Kondo coupling, we observe no breakdown of the composite fermion.

Our results show that the magnetic transition and Kondo breakdown are detached as observed in $\text{Yb}(\text{Rh}_{0.93}\text{Co}_{0.07})_2\text{Si}_2$ [48]. The observed Kondo breakdown corresponds to a modification of the excitation spectra, and does not necessarily translate into a thermodynamic transition. This stands in agreement with the Fradkin-Shenker [30] phase diagram where confined and Higgs phases are adiabatically connected. It would be of great interest to modify the KLM so as to allow for a deconfined phase and probe the full richness of the Fradkin-Shenker phase diagram as suggested in Ref. [27]. On the experimental side, we hope that our results will have an impact on the studies aimed at exploring quantum impurity problems in graphene in a dense situation [49–51].

We thank T. Grover and M. Vojta for many illuminating conversations and Zihong Liu for work on a related project. The authors gratefully acknowledge the Gauss Centre for Supercomputing e.V. (www.gauss-centre.eu) for funding this project by providing computing time on the GCS Supercomputer SUPERMUC-NG at Leibniz Supercomputing Centre (www.lrz.de) as well as through the John von Neumann Institute for Computing (NIC) on the GCS Supercomputer JUWELS [52] at the Jülich Supercomputing Centre (JSC). M.R. is funded by the Deutsche Forschungsgemeinschaft (DFG, German Research Foundation), Project No. 332790403. B.D. thanks the Würzburg-Dresden Cluster of Excellence on Complexity and Topology in Quantum Matter ct.qmat (EXC 2147, project-id 390858490) for financial support. F.F.A. and B.D. acknowledge support from the DFG funded SFB 1170 on Topological and Correlated Electronics at Surfaces and Interfaces.

-
- [1] J. K. Jain, *Composite-fermion approach for the fractional quantum Hall effect*, *Phys. Rev. Lett.* **63**, 199 (1989).
 - [2] T. Giamarchi, *Quantum Physics in One Dimension* (Oxford University Press, 2004).
 - [3] P. Béran, D. Poilblanc, and R. B. Laughlin, *Evidence for composite nature of quasiparticles in the 2D $t - J$ model*, *Nucl. Phys. B* **473**, 707 (1996).
 - [4] F. Grusdt, M. Kánasz-Nagy, A. Bohrdt, C. S. Chiu, G. Ji, M. Greiner, D. Greif, and E. Demler, *Parton theory of magnetic polarons: Mesonic resonances and signatures in dynamics*, *Phys. Rev. X* **8**, 011046 (2018).
 - [5] R. Nandkishore, M. A. Metlitski, and T. Senthil, *Orthogonal metals: The simplest non-Fermi liquids*, *Phys. Rev. B* **86**, 045128 (2012).
 - [6] S. Gazit, F. F. Assaad, and S. Sachdev, *Fermi Surface Reconstruction without Symmetry Breaking*, *Phys. Rev. X* **10**, 041057 (2020).
 - [7] M. Hohenadler and F. F. Assaad, *Fractionalized Metal in a Falicov-Kimball Model*, *Phys. Rev. Lett.* **121**, 086601 (2018).
 - [8] See Supplemental Material, which includes Refs. [53–61] for details of the U(1) gauge theory of the KLM, technical details of the QMC simulations, finite-size scaling analysis of the QMC data, composite fermion spectra at the Γ and Dirac K points, conduction electron spectral functions, as well as large- N and bond fermion mean-field results.
 - [9] D. Withoff and E. Fradkin, *Phase transitions in gapless Fermi systems with magnetic impurities*, *Phys. Rev. Lett.* **64**, 1835 (1990).
 - [10] L. Fritz and M. Vojta, *Phase transitions in the pseudogap Anderson and Kondo models: Critical dimensions, renormalization group, and local-moment criticality*, *Phys. Rev. B* **70**, 214427 (2004).
 - [11] Q. Si, S. Rabello, K. Ingersent, and J. L. Smith, *Locally critical quantum phase transitions in strongly correlated metals*, *Nature (London)* **413**, 804 (2001).
 - [12] P. Coleman, C. Pépin, Q. Si, and R. Ramazashvili, *How do Fermi liquids get heavy and die?* *J. Phys.: Condens. Matter* **13**, R723 (2001).
 - [13] A. Allerdt, A. E. Feiguin, and S. Das Sarma, *Competition between Kondo effect and RKKY physics in graphene magnetism*, *Phys. Rev. B* **95**, 104402 (2017).
 - [14] L. S. Wu, W. J. Gannon, I. A. Zaliznyak, A. M. Tsvetlik, M. Brockmann, J.-S. Caux, M. S. Kim, Y. Qiu, J. R. D. Copley, G. Ehlers, A. Podlesnyak, and M. C. Aronson, *Orbital-exchange and fractional quantum number excitations in an f -electron metal*, $\text{Yb}_2\text{Pt}_2\text{Pb}$, *Science* **352**, 1206 (2016).
 - [15] B. Danu, M. Vojta, F. F. Assaad, and T. Grover, *Kondo Breakdown in a Spin-1/2 Chain of Adatoms on a Dirac Semimetal*, *Phys. Rev. Lett.* **125**, 206602 (2020).
 - [16] S. Paschen, T. Lühmann, S. Wirth, P. Gegenwart, O. Trovarelli, C. Geibel, F. Steglich, P. Coleman, and Q. Si, *Hall-effect evolution across a heavy-fermion quantum critical point*, *Nature (London)* **432**, 881 (2004).
 - [17] S. Friedemann, N. Oeschler, S. Wirth, C. Krellner, C. Geibel, F. Steglich, S. Paschen, S. Kirchner, and Q. Si, *Fermi-surface collapse and dynamical scaling near a quantum-critical point*, *Proc. Natl. Acad. Sci. U.S.A.* **107**, 14547 (2010).

- [18] L. Prochaska, X. Li, D. C. MacFarland, A. M. Andrews, M. Bonta, E. F. Bianco, S. Yazdi, W. Schrenk, H. Detz, A. Limbeck, Q. Si, E. Ringe, G. Strasser, J. Kono, and S. Paschen, *Singular charge fluctuations at a magnetic quantum critical point*, *Science* **367**, 285 (2020).
- [19] N. Maksimovic, D. H. Eilbott, T. Cookmeyer, F. Wan, J. Rusz, V. Nagarajan, S. C. Haley, E. Maniv, A. Gong, S. Faubel, I. M. Hayes, A. Bangura, J. Singleton, J. C. Palmstrom, L. Winter, R. McDonald, S. Jang, P. Ai, Y. Lin, S. Ciocys, J. Gobbo, Y. Werman, P. M. Oppeneer, E. Altman, A. Lanzara, and J. G. Analytis, *Evidence for a delocalization quantum phase transition without symmetry breaking in CeCoIn₅*, *Science* **375**, 76 (2022).
- [20] M. Vojta, *Orbital-Selective Mott Transitions: Heavy Fermions and Beyond*, *J. Low Temp. Phys.* **161**, 203 (2010).
- [21] M. Oshikawa, *Topological Approach to Luttinger's Theorem and the Fermi Surface of a Kondo Lattice*, *Phys. Rev. Lett.* **84**, 3370 (2000).
- [22] T. Senthil, S. Sachdev, and M. Vojta, *Fractionalized Fermi Liquids*, *Phys. Rev. Lett.* **90**, 216403 (2003).
- [23] J. S. Hofmann, F. F. Assaad, and T. Grover, *Fractionalized Fermi liquid in a frustrated Kondo lattice model*, *Phys. Rev. B* **100**, 035118 (2019).
- [24] S. J. Yamamoto and Q. Si, *Fermi Surface and Antiferromagnetism in the Kondo Lattice: An Asymptotically Exact Solution in $d > 1$ Dimensions*, *Phys. Rev. Lett.* **99**, 016401 (2007).
- [25] N. Read and D. M. Newns, *On the solution of the Coqblin-Schrieffer Hamiltonian by the large- N expansion technique*, *J. Phys. C* **16**, 3273 (1983).
- [26] A. Auerbach and K. Levin, *Kondo Bosons and the Kondo Lattice: Microscopic Basis for the Heavy Fermi Liquid*, *Phys. Rev. Lett.* **57**, 877 (1986).
- [27] S. Saremi and P. A. Lee, *Quantum critical point in the Kondo-Heisenberg model on the honeycomb lattice*, *Phys. Rev. B* **75**, 165110 (2007).
- [28] M. Raczkowski and F. F. Assaad, *Emergent Coherent Lattice Behavior in Kondo Nanosystems*, *Phys. Rev. Lett.* **122**, 097203 (2019).
- [29] B. Danu, F. F. Assaad, and F. Mila, *Exploring the Kondo Effect of an Extended Impurity with Chains of Co Adatoms in a Magnetic Field*, *Phys. Rev. Lett.* **123**, 176601 (2019).
- [30] E. Fradkin and S. H. Shenker, *Phase diagrams of lattice gauge theories with Higgs fields*, *Phys. Rev. D* **19**, 3682 (1979).
- [31] S. Burdin, A. Georges, and D. R. Grempel, *Coherence Scale of the Kondo Lattice*, *Phys. Rev. Lett.* **85**, 1048 (2000).
- [32] D. K. Morr, *Theory of scanning tunneling spectroscopy: from Kondo impurities to heavy fermion materials*, *Rep. Prog. Phys.* **80**, 014502 (2017).
- [33] B. Danu, Z. Liu, F. F. Assaad, and M. Raczkowski, *Zooming in on heavy fermions in Kondo lattice models*, *Phys. Rev. B* **104**, 155128 (2021).
- [34] T. A. Costi, *Kondo Effect in a Magnetic Field and the Magnetoresistivity of Kondo Alloys*, *Phys. Rev. Lett.* **85**, 1504 (2000).
- [35] M. Maltseva, M. Dzero, and P. Coleman, *Electron Co-tunneling into a Kondo Lattice*, *Phys. Rev. Lett.* **103**, 206402 (2009).
- [36] L. Borda, L. Fritz, N. Andrei, and G. Zaránd, *Theory of inelastic scattering from quantum impurities*, *Phys. Rev. B* **75**, 235112 (2007).
- [37] F. F. Assaad, M. Bercx, F. Goth, A. Götz, J. S. Hofmann, E. Huffman, Z. Liu, F. P. Toldin, J. S. E. Portela, and J. Schwab, *The ALF (Algorithms for Lattice Fermions) project release 2.0. Documentation for the auxiliary-field quantum Monte Carlo code*, *SciPost Phys. Codebases*, **1** (2022).
- [38] R. Blankenbecler, D. J. Scalapino, and R. L. Sugar, *Monte Carlo calculations of coupled boson-fermion systems. I*, *Phys. Rev. D* **24**, 2278 (1981).
- [39] G. Sugiyama and S. Koonin, *Auxiliary field Monte-Carlo for quantum many-body ground states*, *Ann. Phys. (NY)* **168**, 1 (1986).
- [40] S. R. White, D. J. Scalapino, R. L. Sugar, E. Y. Loh, J. E. Gubernatis, and R. T. Scalettar, *Numerical study of the two-dimensional Hubbard model*, *Phys. Rev. B* **40**, 506 (1989).
- [41] S. Sorella, S. Baroni, R. Car, and M. Parrinello, *A Novel Technique for the Simulation of Interacting Fermion Systems*, *Europhys. Lett.* **8**, 663 (1989).
- [42] F. F. Assaad and H. Evertz, in *Computational Many-Particle Physics*, Lecture Notes in Physics, Vol. 739, edited by H. Fehske, R. Schneider, and A. Weiße (Springer, Berlin Heidelberg, 2008) pp. 277–356.
- [43] F. F. Assaad, *Quantum Monte Carlo Simulations of the Half-Filled Two-Dimensional Kondo Lattice Model*, *Phys. Rev. Lett.* **83**, 796 (1999).
- [44] S. Capponi and F. F. Assaad, *Spin and charge dynamics of the ferromagnetic and antiferromagnetic two-dimensional half-filled Kondo lattice model*, *Phys. Rev. B* **63**, 155114 (2001).
- [45] M. Raczkowski and F. F. Assaad, *Phase diagram and dynamics of the SU(N) symmetric Kondo lattice model*, *Phys. Rev. Research* **2**, 013276 (2020).
- [46] Y. Zhong, K. Liu, W. Yu-Feng, Y.-Q. Wang, and H.-G. Luo, *Half-filled Kondo lattice on the honeycomb lattice*, *Eur. Phys. J. B* **86**, 195 (2013).
- [47] G.-M. Zhang and L. Yu, *Kondo singlet state coexisting with antiferromagnetic long-range order: A possible ground state for Kondo insulators*, *Phys. Rev. B* **62**, 76 (2000).
- [48] S. Friedemann, T. Westerkamp, M. Brando, N. Oeschler, S. Wirth, P. Gegenwart, C. Krellner, C. Geibel, and F. Steglich, *Detaching the antiferromagnetic quantum critical point from the Fermi-surface reconstruction in YbRh₂Si₂*, *Nat. Phys.* **5**, 465 (2009).
- [49] L. Fritz and M. Vojta, *The physics of Kondo impurities in graphene*, *Rep. Prog. Phys.* **76**, 032501 (2013).
- [50] Y. Jiang, P.-W. Lo, D. May, G. Li, G.-Y. Guo, F. B. Anders, T. Taniguchi, K. Watanabe, J. Mao, and E. Y. Andrei, *Inducing Kondo screening of vacancy magnetic moments in graphene with gating and local curvature*, *Nat. Commun.* **9**, 2349 (2018).
- [51] J. Hwang, K. Kim, H. Ryu, J. Kim, J.-E. Lee, S. Kim, M. Kang, B.-G. Park, A. Lanzara, J. Chung, S.-K. Mo, J. Denlinger, B. I. Min, and C. Hwang, *Emergence of Kondo Resonance in Graphene Intercalated with Cerium*, *Nano Lett.* **18**, 3661 (2018).
- [52] Jülich Supercomputing Centre, *JUWELS: Modular Tier-0/1 Supercomputer at the Jülich Supercomputing Centre*, *J. Large-Scale Res. Facil.* **5**, A135 (2019).
- [53] J. W. Negele and H. Orland, *Quantum Many-particle Systems* (Westview Press, 1998).

- [54] T. Hazra and P. Coleman, *Luttinger sum rules and spin fractionalization in the $SU(N)$ Kondo lattice*, [Phys. Rev. Research **3**, 033284 \(2021\)](#).
- [55] C. Wu and S.-C. Zhang, *Sufficient condition for absence of the sign problem in the fermionic quantum Monte Carlo algorithm*, [Phys. Rev. B **71**, 155115 \(2005\)](#).
- [56] T. Sato, F. F. Assaad, and T. Grover, *Quantum Monte Carlo Simulation of Frustrated Kondo Lattice Models*, [Phys. Rev. Lett. **120**, 107201 \(2018\)](#).
- [57] K. S. D. Beach, *Identifying the maximum entropy method as a special limit of stochastic analytic continuation*, [arXiv:cond-mat/0403055 \(2004\)](#).
- [58] S. M. Chester, W. Landry, J. Liu, D. Poland, D. Simmons-Duffin, N. Su, and A. Vichi, *Bootstrapping Heisenberg magnets and their cubic instability*, [Phys. Rev. D **104**, 105013 \(2021\)](#).
- [59] H. Watanabe and M. Ogata, *Fermi-Surface Reconstruction without Breakdown of Kondo Screening at the Quantum Critical Point*, [Phys. Rev. Lett. **99**, 136401 \(2007\)](#).
- [60] C. Jurecka and W. Brenig, *Bond-operator mean-field theory of the half-filled Kondo lattice model*, [Phys. Rev. B **64**, 092406 \(2001\)](#).
- [61] R. Eder and P. Wróbel, *Antiferromagnetic phase of the Kondo insulator*, [Phys. Rev. B **98**, 245125 \(2018\)](#).

Supplemental Material for:
Breakdown of heavy quasiparticles in a honeycomb Kondo lattice:
A quantum Monte Carlo study

AUXILIARY FIELD QMC AND U(1) GAUGE THEORY OF THE KONDO LATTICE MODEL

To at best understand the phases of the Kondo lattice model,

$$\hat{H}_{KLM} = \sum_{i,j} T_{i,j} \hat{c}_i^\dagger \hat{c}_j + \frac{J_k}{2} \sum_i \hat{c}_i^\dagger \boldsymbol{\sigma} \hat{c}_i \cdot \hat{\mathbf{S}}_i, \quad (\text{S1})$$

where $\hat{c}_i^\dagger = (\hat{c}_{i,\uparrow}^\dagger, \hat{c}_{i,\downarrow}^\dagger)$ is a Wannier-state spinor, we adopt an Abrikosov representation of the spin operator, $\hat{\mathbf{S}}_i = \frac{1}{2} \hat{\mathbf{f}}_i^\dagger \boldsymbol{\sigma} \hat{\mathbf{f}}_i$ with $\hat{\mathbf{f}}_i^\dagger = (\hat{f}_{i,\uparrow}^\dagger, \hat{f}_{i,\downarrow}^\dagger)$ and constraint $\hat{\mathbf{f}}_i^\dagger \hat{\mathbf{f}}_i = 1$. In the constrained Hilbert space, the identity:

$$\frac{J_k}{2} \hat{c}_i^\dagger \boldsymbol{\sigma} \hat{c}_i \cdot \hat{\mathbf{S}}_i = -\frac{J_k}{4} (\hat{V}_i^\dagger \hat{V}_i + \hat{V}_i \hat{V}_i^\dagger) \quad (\text{S2})$$

with $\hat{V}_i^\dagger = \hat{c}_i^\dagger \hat{\mathbf{f}}_i$ holds. To proceed we relax the constraint and consider the Hamiltonian

$$\hat{H}_{KLM} = \lim_{U \rightarrow \infty} \left\{ \sum_{i,j} T_{i,j} \hat{c}_i^\dagger \hat{c}_j - \frac{J_k}{8} \sum_i \left([\hat{V}_i^\dagger + \hat{V}_i]^2 + [i\hat{V}_i^\dagger - i\hat{V}_i]^2 \right) + \frac{U}{2} \sum_i (\hat{\mathbf{f}}_i^\dagger \hat{\mathbf{f}}_i - 1)^2 \right\}. \quad (\text{S3})$$

Since the Hubbard term commutes with the Hamiltonian, the projection onto the physical Hilbert space occurs at a rate set by $\left\langle (\hat{\mathbf{f}}_i^\dagger \hat{\mathbf{f}}_i - 1)^2 \right\rangle \propto e^{-\beta U/2}$, where β corresponds to the inverse temperature. Using the Trotter decomposition, and Hubbard Stratonovich transformation to decouple the perfect square terms we obtain the following form for the grand-canonical partition function [53]:

$$Z = \text{Tre}^{-\beta \hat{H}_{KLM}} \propto \int D \left\{ \mathbf{f}_i^\dagger(\tau), \mathbf{f}_i(\tau), \mathbf{c}_i^\dagger(\tau), \mathbf{c}_i(\tau), b_i(\tau), a_{0,i}(\tau) \right\} e^{-S} \quad (\text{S4})$$

with

$$S = \int_0^\beta d\tau \left\{ \sum_i \left[\frac{N}{J_k} |b_i(\tau)|^2 + \frac{N}{U} |a_{0,i}(\tau)|^2 + i \frac{N}{2} a_{0,i}(\tau) + \mathbf{f}_i^\dagger(\tau) [\partial_\tau - i a_{0,i}(\tau)] \mathbf{f}_i(\tau) + b_i(\tau) \mathbf{c}_i^\dagger \mathbf{f}_i + \overline{b_i(\tau)} \mathbf{f}_i^\dagger \mathbf{c}_i \right] + \sum_{i,j} \mathbf{c}_i^\dagger(\tau) [\partial_\tau \delta_{i,j} + T_{i,j}] \mathbf{c}_j(\tau) \right\}. \quad (\text{S5})$$

In the above, $a_{0,i}(\tau)$ is a real field used to impose the constraint, $b_i(\tau)$ a complex field for the Kondo term, and \mathbf{c}_i^\dagger as well as \mathbf{f}_i^\dagger are spinors of Grassmann variables. We have also taken the liberty of enhancing the spin index from $N = 2$ to a general N with constraint $\mathbf{f}_i^\dagger \mathbf{f}_i = N/2$ [45, 54]. The above action is the starting point for auxiliary field QMC simulations [37] as well as for the classification of phases. For the QMC simulations we use the Gauss-Hermite quadrature to replace continuous fields by discrete ones. The integration over the Grassmann variables yields the fermion determinant, that for particle-hole symmetric conduction electrons and even values of N is positive semi-definite. The integration over the Hubbard-Stratonovich fields is then carried out with Monte Carlo importance sampling. For details of the implementation, we refer the reader to Ref. [37]. In particular for the calculation presented here, we have used the implementation of the Kondo lattice model of the ALF-2.0 library.

The constraint leads to a U(1) local gauge invariance. In particular, and only in the $U \rightarrow \infty$ limit, the canonical transformation

$$\mathbf{f}_i(\tau) \rightarrow \mathbf{f}_i(\tau) e^{i\chi_i(\tau)} \quad (\text{S6})$$

amounts to redefining the fields

$$a_{0,i}(\tau) \rightarrow a_{0,i}(\tau) + \partial_\tau \chi_i(\tau) \quad \text{and} \quad b_i(\tau) \rightarrow b_i(\tau) e^{-i\chi_i(\tau)} \quad (\text{S7})$$

in the action.

PHASES OF THE KONDO LATTICE MODEL

The above action allows us to define precisely the two phases of the Kondo lattice model that are of importance to us in the present article. The spin-density-wave (SDW) phase is characterized by long ranged order in

$$\langle \frac{1}{2} \hat{\mathbf{f}}_i^\dagger \boldsymbol{\sigma} \hat{\mathbf{f}}_i \cdot \frac{1}{2} \hat{\mathbf{f}}_j^\dagger \boldsymbol{\sigma} \hat{\mathbf{f}}_j \rangle \quad (\text{S8})$$

and is hence characterized by a non-vanishing vacuum expectation value of $\langle \frac{1}{2} \hat{\mathbf{f}}_i^\dagger \boldsymbol{\sigma} \hat{\mathbf{f}}_i \rangle$ in the thermodynamic limit characteristic of spontaneous symmetry breaking of the global SU(2) spin symmetry. Note that the above expectation value is taken with respect to the action of Eq. (S5).

The Kondo phase is more subtle to define since it is not characterized by a broken symmetry. Let $b_i(\tau) = |b_i(\tau)| e^{i\varphi_i(\tau)}$ and

$$\tilde{\mathbf{f}}_i(\tau) = e^{i\varphi_i(\tau)} \mathbf{f}_i(\tau). \quad (\text{S9})$$

$\tilde{\mathbf{f}}_i$ is a physical fermion operator. As mentioned above, under a local U(1) gauge transformation, $\mathbf{f}_i \rightarrow \mathbf{f}_i e^{i\chi_i(\tau)}$, $\varphi_i(\tau) \rightarrow \varphi_i(\tau) - \chi_i(\tau)$ such that $\tilde{\mathbf{f}}_i$ remains invariant. It hence carries no gauge charge. $\tilde{\mathbf{f}}_i$ carries electric charge. Consider the global U(1) charge transformation, $\hat{T}(\alpha) = e^{i\alpha \sum_i \hat{c}_i^\dagger \hat{c}_i}$. Since $T(\alpha)$ is a conserved quantity, and the physical electron transforms as $\hat{T}(\alpha)^{-1} \hat{c}_i \hat{T}(\alpha) = e^{i\alpha} \hat{c}_i$, the phase $\varphi_i(\tau)$ transforms as $\varphi_i(\tau) \rightarrow \varphi_i(\tau) + \alpha$. Hence $\tilde{\mathbf{f}}_i$ transforms as the electron: $\tilde{\mathbf{f}}_i \rightarrow \tilde{\mathbf{f}}_i e^{i\alpha}$. In the heavy fermion phase, the electron operator $\tilde{\mathbf{f}}_i$ emerges as a new particle excitation that acquires coherence. This is what is meant in colloquial terms by *the spins delocalize and participate in the Luttinger volume*.

Since in the heavy fermions phase $\tilde{\mathbf{f}}_i$ is the emergent quasiparticle, it is natural to write the action for this degree of freedom. From Eq. (S5) and in the limit $U \rightarrow \infty$, one readily obtains:

$$S = \int_0^\beta d\tau \left\{ \sum_i \left[\frac{N}{J_k} |b_i(\tau)|^2 + i \frac{N}{2} a_{0,i}(\tau) + \tilde{\mathbf{f}}_i^\dagger(\tau) [\partial_\tau - i a_{0,i}(\tau) - i \partial_\tau \varphi_i(\tau)] \tilde{\mathbf{f}}_i(\tau) + |b_i(\tau)| \left(\mathbf{c}_i^\dagger \tilde{\mathbf{f}}_i + \tilde{\mathbf{f}}_i^\dagger \mathbf{c}_i \right) \right] + \sum_{i,j} \mathbf{c}_i^\dagger(\tau) [\partial_\tau \delta_{i,j} + T_{i,j}] \mathbf{c}_j(\tau) \right\}. \quad (\text{S10})$$

Importantly, $\tilde{\mathbf{f}}_i(\tau)$ does not possess a local U(1) gauge charge such that $\langle \tilde{\mathbf{f}}_i^\dagger(\tau) \tilde{\mathbf{f}}_j(\tau') \rangle$ does not vanish by symmetry for $(i, \tau) \neq (j, \tau')$. In contrast, owing to the local U(1) symmetry, $\langle \mathbf{f}_i^\dagger(\tau) \mathbf{f}_j(\tau') \rangle = 0$ if $(i, \tau) \neq (j, \tau')$.

Since in the Kondo phase $\tilde{\mathbf{f}}_i$ is the emergent low lying quasiparticle, we expect the phase $\varphi_i(\tau)$ to vary slowly in time. This freezing out of the dynamics of the gauge field corresponds to the Higgs mechanism. Here φ drops out from the action and the relevant theory is that of interacting c and \tilde{f} electrons which is very reminiscent of the physics of the periodic Anderson model. This formalizes the accepted notion that the Kondo lattice model shares the very same physics as the periodic Anderson model in the local moment regime. If the ground state turns out to be a Fermi liquid, then Luttinger theorem should apply and both electron species should be included in the Luttinger count. In the Higgs phase, φ , is stuck in a gauge choice, say $\varphi = 0$. Hence there is no distinction between the $\tilde{\mathbf{f}}_i(\tau)$ and $\mathbf{f}_i(\tau)$. In other words, the Abrikosov fermion loses its gauge charge and acquires an physical electric one. In this sense we have for the Kondo phase

$$\langle b_i(\tau) \rangle \propto \langle \mathbf{f}_i^\dagger(\tau) \mathbf{c}_i(\tau) \rangle \neq 0. \quad (\text{S11})$$

Let us note that in any exact evaluation of the partition function – as carried out in our Monte Carlo simulations – $\langle \mathbf{f}_i^\dagger(\tau) \mathbf{c}_i(\tau) \rangle$ vanishes identically. However, the measurement of $\langle e^{-i\varphi_i(\tau)} \mathbf{f}_i^\dagger(\tau) \mathbf{c}_i(\tau) \rangle$ is finite and captures the hybridization matrix element characteristic of large- N mean-field theories.

We now argue that, at least in the large- N limit, $\tilde{\mathbf{f}}_i$ corresponds to the composite fermion operator. Including amplitude fluctuations we have:

$$\tilde{\mathbf{f}}_i \propto b_i(\tau) \mathbf{f}_i(\tau) \propto \left[\mathbf{f}_i^\dagger(\tau) \mathbf{c}_i(\tau) \right] \mathbf{f}_i(\tau). \quad (\text{S12})$$

The above is precisely the form of the composite fermion operator, considered in this article, in the large- N limit [33].

We are now in a position to define precisely the relevant phases of the KLM that we encounter in this article. They are summarized in Table I.

Phases	$\langle \mathbf{f}_i^\dagger \boldsymbol{\sigma} \mathbf{f}_i \rangle$	$\langle b_i(\tau) \rangle$
SDW	✓	×
Kondo	×	✓
Kondo+SDW	✓	✓

TABLE I. SDW, Kondo and Kondo+SDW phases of the Kondo lattice model. ✓ (×) refers to a non-vanishing (vanishing) value of the order parameter.

SUPPLEMENTAL QMC RESULTS

QMC setup

The approach relies on the U(1) gauge formulation of the KLM described above. The integration over the Grassmann variables yields the fermion determinant. For the particle-hole symmetric conduction band, one will readily show, that it is positive semi-definite [55, 56]. To formulate the algorithm, we discretize the imaginary time and choose $\Delta\tau t = 0.2$ ($\Delta\tau t = 0.1$) on the honeycomb (square) lattice and use the Gauss-Hermite quadrature to discretize the fields.

We have used a projective version of the QMC algorithm based on the imaginary time evolution of a trial wave function $|\Psi_T\rangle$, with $\langle \Psi_T | \Psi_0 \rangle \neq 0$, to the ground state $|\Psi_0\rangle$:

$$\frac{\langle \Psi_0 | \hat{O} | \Psi_0 \rangle}{\langle \Psi_0 | \Psi_0 \rangle} = \lim_{\Theta \rightarrow \infty} \frac{\langle \Psi_T | e^{-\Theta \hat{H}} \hat{O} e^{-\Theta \hat{H}} | \Psi_T \rangle}{\langle \Psi_T | e^{-2\Theta \hat{H}} | \Psi_T \rangle}. \quad (\text{S13})$$

Since the energy scale of the RKKY interaction scales as J_k^2 , convergence to the magnetically ordered ground state in the weak coupling requires adequately increased projection parameters, i.e., $\Theta t = 40$ at $J_k/t = 0.8$ and $\Theta t = 160$ at $J_k/t = 0.4$ on the honeycomb lattice. On the other hand, on the square lattice $\Theta t = 80$ was found to be already sufficient down to $J_k/t = 0.2$.

For the analytical continuation, we have made use of the stochastic Maximum Entropy method [57] implemented in the ALF-library.

Magnetic order-disorder transition

In order to determine the precise location of the magnetic order-disorder transition, we calculate the spin structure factor for the f spins

$$S^f(\mathbf{k}) = \frac{4}{L^2} \sum_{\delta=A,B} \sum_{\mathbf{r}} e^{i\mathbf{k}\cdot\mathbf{r}} \langle \hat{\mathbf{S}}_\delta(\mathbf{r}) \cdot \hat{\mathbf{S}}_\delta \rangle, \quad (\text{S14})$$

from which we construct the renormalization group invariant correlation ratio

$$R_f = 1 - \frac{S^f(\mathbf{Q} + \delta\mathbf{k})}{S^f(\mathbf{Q})}, \quad (\text{S15})$$

where $\mathbf{Q} = (0, 0)$ is the ordering wavevector and $\delta\mathbf{k}$ is the smallest wavevector on the $L \times L$ honeycomb lattice. As can be seen in Fig. S1, R_f scales to unity (zero) for ordered (disordered) states and shows a crossing point as a function of system size at the critical point J_k^c . Given that the charge degrees of freedom are gapped across the transition, we expect that it belongs to the universality class of the 3D classical Heisenberg (O(3)) model. Indeed, assuming the correlation length exponent $1/\nu = 1.40511(6)$ [58] of the latter and using the scaling assumption

$$R_f = f[(J_k/J_k^c - 1)L^{1/\nu}], \quad (\text{S16})$$

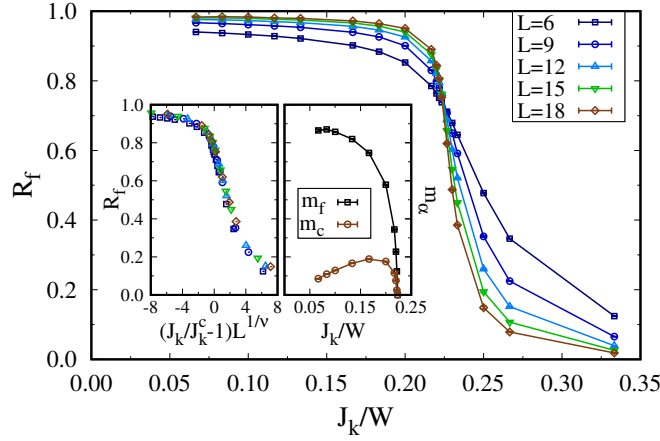


FIG. S1. Correlation ratio R_f defined in Eq. (S15) as a function of J_k/W . Left inset shows the scaling collapse of R_f for $L \geq 12$ assuming the critical exponent $1/\nu = 1.40511(6)$ of the 3D classical Heisenberg (O(3)) model [58]. Right inset shows the staggered magnetic moment $m_{\alpha=\{c,f\}}$ in the thermodynamic limit.

we obtain for $L \geq 12$ a good quality data collapse of R_f shown in the left inset of Fig. S1. It allows us to estimate $J_k^c/W = 0.2227(3)$.

As shown in Fig. S2, we have equally performed finite-size scaling of both $S^f(\mathbf{Q})$ and the spin structure factor for the conduction electron spins

$$S^c(\mathbf{Q}) = \frac{1}{L^2} \sum_{\delta=A,B} \sum_{\mathbf{r}} e^{i\mathbf{Q}\cdot\mathbf{r}} \langle \hat{\mathbf{c}}_{\delta}^{\dagger}(\mathbf{r}) \boldsymbol{\sigma} \hat{\mathbf{c}}_{\delta}(\mathbf{r}) \cdot \hat{\mathbf{c}}_{\delta}^{\dagger} \boldsymbol{\sigma} \hat{\mathbf{c}}_{\delta} \rangle. \quad (\text{S17})$$

We have used linear [Fig. S2(a)] and second-order [Fig. S2(b)] polynomial forms in $1/L$. The resultant orbital $\alpha = \{c, f\}$ resolved staggered magnetic moments

$$m_{\alpha} = \sqrt{\lim_{L \rightarrow \infty} \frac{S^{\alpha}(\mathbf{Q})}{2L^2}} \quad (\text{S18})$$

both scale continuously to zero at $J_k^c/W = 0.223(1)$ (see the right inset of Fig. S1) which matches perfectly the previously extracted critical point $J_k^c/W = 0.2227(3)$. We note that the good agreement between the extrapolation with an analytical form in $1/L$ and the data collapse based on the correlation ratio R_f can be ascribed to the very small anomalous dimension of 3D O(3) criticality.

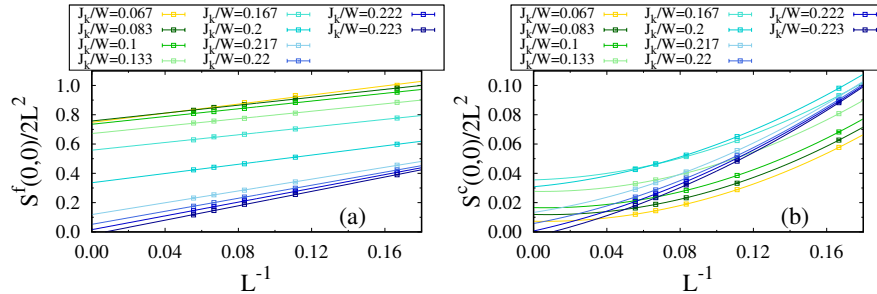


FIG. S2. Finite-size extrapolation of the antiferromagnetic spin structure factor at $\mathbf{Q} = (0,0)$ on the honeycomb KLM for the (a) f - and (b) c -electrons on approaching the magnetic order-disorder transition point; solid lines are linear and second-order polynomial fits to the QMC data.

Conduction electron spectral function

Figure S3 plots the conduction electron spectral function, $A_c(\mathbf{k}, \omega) = -\frac{1}{\pi} \text{Im} G_c^{ret}(\mathbf{k}, \omega)$, where

$$G_c^{ret}(\mathbf{k}, \omega) = -i \int_0^\infty dt e^{i\omega t} \sum_\sigma \langle \{ \hat{c}_{\mathbf{k},\sigma}(t), \hat{c}_{\mathbf{k},\sigma}^\dagger(0) \} \rangle \quad (\text{S19})$$

from the stochastic analytical continuation of the QMC data generated on the $L = 18$ honeycomb KLM.

In the region of the phase diagram with active Kondo screening, the composite fermion and conduction electron operators share the same quantum numbers. Thus their single particle spectral functions shall have identical supports both revealing the low energy composite fermion bands. However, the corresponding quasiparticle poles of the conduction electron Green's function carry much less spectral weight such that $A_c(\mathbf{k}, \omega)$ exhibits relatively faint bands, see Figs. S3(a) and S3(b). Moreover, since the quasiparticle residue in the small J_k/W limit tracks the Kondo scale $Z_{\mathbf{k}} \simeq e^{-W/J_k}$, resolving composite quasiparticles in Fig. S3(c) requires a logarithmic scale as the spectral weight is nearly fully exhausted by two bands separated by a small gap at the Dirac point K but otherwise closely reminiscent of the tight binding band structure of the honeycomb lattice.

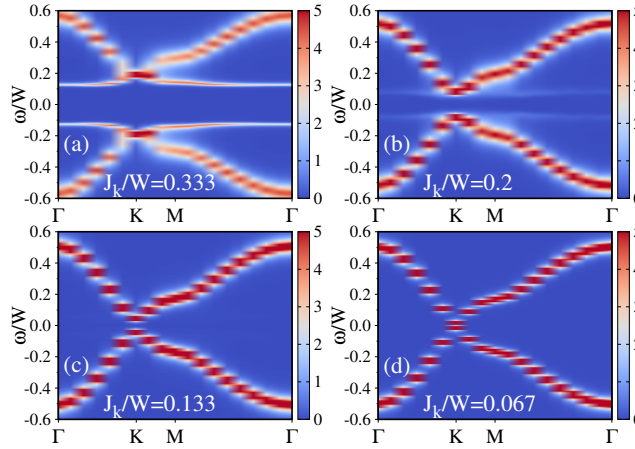


FIG. S3. Same as in Fig. 2 in the main text but for the conduction electrons.

Quasiparticle residue $Z_{\mathbf{k}}^\psi$ and single particle gap $\Delta_{qp}(\mathbf{k})$

The behavior of the imaginary time composite fermion Green's function $G_\psi(\mathbf{k}, \tau)$ at large times, $G(\mathbf{k}, \tau) \xrightarrow{\tau \rightarrow \infty} Z_{\mathbf{k}} e^{-\Delta_{qp}(\mathbf{k})\tau}$, allows one to extract the quasiparticle residue $Z_{\mathbf{k}}^\psi$ and the corresponding single particle gap $\Delta_{qp}(\mathbf{k})$ without the need of analytical continuation. Figure S4 shows the finite-size scaling analysis of the resultant QMC data which led us to the J_k/W -dependence of the quasiparticle residue $Z_{\mathbf{k}}^\psi$ and the corresponding single particle gap $\Delta_{qp}(\mathbf{k})$ at the Γ and Dirac K points (honeycomb lattice) as well as at the M point (square lattice) presented in the main text.

Figure S5(a) illustrates the behavior of the composite fermion spectral function $A_\psi(\mathbf{k}, \omega)$ at the Γ and Dirac K points for different values of Kondo coupling J_k/W . The corresponding density of states $A_\psi(\omega) = \frac{1}{L^2} \sum_{\mathbf{k}} A_\psi(\mathbf{k}, \omega)$ is shown in Fig. S5(b).

As can be seen, in the Kondo insulating phase at $J_k/W = 0.233$, coherent Kondo screening results in a well-defined peak at the Γ momentum which determines the minimal gap. The latter is also seen in $A_\psi(\omega)$ since the flat band of composite fermion quasiparticles generates a sharp peak that flanks the gap. The low energy part of $A_\psi(\mathbf{k}, \omega)$ evolves smoothly across the magnetic order-disorder transition at $J_k^c/W = 0.2227(3)$ with a gradual shift of the minimal gap from the Γ point to the Dirac K point. As is apparent, the change in the position of the minimal gap takes place away from J_k^c . Assuming a rigid band shift, the switch of Fermi wavevector in the metallic state at small dopings would lead to a change in the Fermi surface topology (Lifshitz transition). Note however that this change in topology of the Fermi surface is unrelated to the breakdown of Kondo screening [59].

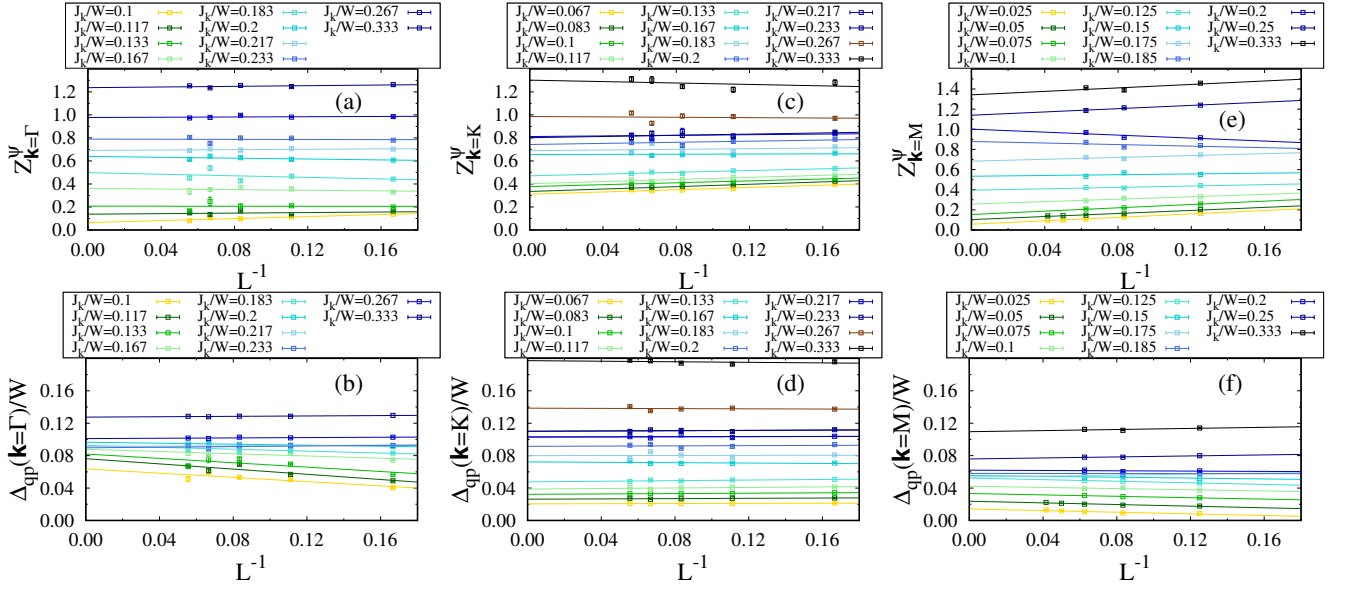


FIG. S4. Finite-size extrapolation of the quasiparticle residue $Z_{\mathbf{k}}^{\psi}$ (top) and the corresponding single particle gap $\Delta_{qp}(\mathbf{k})$ (bottom) extracted from the imaginary-time composite fermion Green's function $G_{\psi}(\mathbf{k}, \tau)$ at the (a,b) $\Gamma = (0,0)$ and (c,d) Dirac $K = (\frac{4\pi}{3}, 0)$ points on the honeycomb KLM and at the (e,f) $M = (\pi, \pi)$ point on the square KLM. Solid lines are linear in $1/L$ fits to the QMC data.

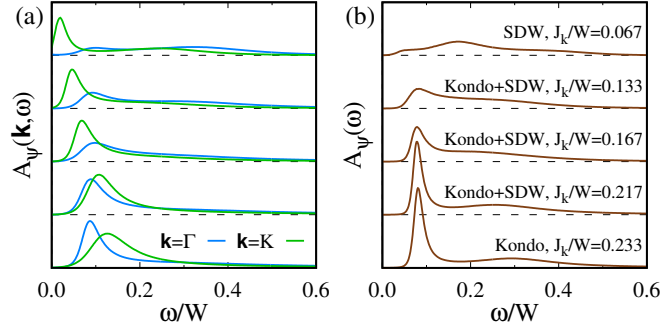


FIG. S5. (a) Composite fermion spectral function $A_{\psi}(\mathbf{k}, \omega)$ at the Γ and Dirac K points and (b) the corresponding density of states $A_{\psi}(\omega) = \frac{1}{L^2} \sum_{\mathbf{k}} A_{\psi}(\mathbf{k}, \omega)$ with decreasing (from bottom to top) Kondo coupling J_k obtained on the $L = 18$ honeycomb KLM.

As long as the magnetic order and low energy composite fermion band coexist (Kondo+SDW phase), one can track the signature of the quasiparticle band in $A_{\psi}(\omega)$. This should be contrasted with the SDW phase where in the absence of Kondo screening, signaled by a broad featureless spectrum at the Γ point, an appropriate approach is the large- S picture. It accounts for the observed rearrangement of $A_{\psi}(\omega)$ such that a dominant contribution occurs at $\omega/W \simeq 1/6$. It reflects the van Hove singularity in the conduction electron density of states.

Local spin-spin correlation function S^{cf}

Figure S6 shows finite-size scaling of the local spin-spin correlation function

$$S^{cf} = \frac{2}{3N} \sum_i \langle \hat{c}_i^\dagger \sigma \hat{c}_i \cdot \hat{S}_i \rangle \quad (\text{S20})$$

which led us to the J_k/W -dependence of this quantity presented in the main text.

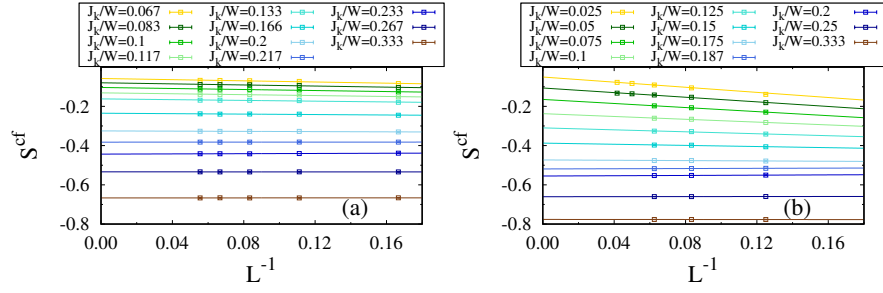


FIG. S6. Finite-size extrapolation of the local spin-spin correlation function $S^{cf} = \frac{2}{3N} \sum_i \langle \hat{c}_i^\dagger \boldsymbol{\sigma} \hat{c}_i \cdot \hat{\mathbf{S}}_i \rangle$ for the (a) honeycomb and (b) square KLMS. Solid lines are linear in $1/L$ fits to the QMC data.

MEAN-FIELD APPROXIMATIONS

In this section, we review mean-field approximations in the aim of providing an account of our results. We will see that both the large- N as well as the bond fermion mean-field approximations fail at providing *consistent* results for the square and honeycomb lattices.

In the large- N mean-field approximation we neglect the fluctuations of the boson field $b_i(\tau)$ and take into account the constraint on average. The field $b_i(\tau)$ possesses phase as well as amplitude fluctuations. Phase fluctuations will not be taken into account at the mean-field level and the only manner in which Kondo breakdown can occur is through the vanishing of the amplitude of the boson field. This actually stands at odds with our QMC data that suggest that the amplitude of the field remains constant for all values of the Kondo coupling and that Kondo breakdown occurs due to phase fluctuations. In the single impurity limit, or equivalently in the absence of magnetic ordering, this approach does capture the differences between the honeycomb and square lattices, see Fig. S7. However, when magnetic ordering, alongside Kondo screening is included, the approximation yields *Kondo breakdown* in the magnetic phase for *both* the honeycomb (see Fig. S8 and also Ref. [46]) and square [44, 47] lattices.

An approximation that captures the coexistence of Kondo screening and magnetism on the square lattice, is the bond fermion mean-field approximation [60, 61]. In this strong coupling approach, the Kondo effect is accounted for by a vacuum expectation value of the the singlet correlator, $\hat{s}_i^\dagger = \frac{1}{\sqrt{2}} (\hat{c}_{i,\uparrow}^\dagger \hat{f}_{i,\downarrow}^\dagger - \hat{c}_{i,\downarrow}^\dagger \hat{f}_{i,\uparrow}^\dagger)$. Since $\langle |b_i|^2 \rangle \propto \langle \hat{V}_i^\dagger \hat{V}_i \rangle \propto \langle \frac{1}{2} \hat{c}_i^\dagger \boldsymbol{\sigma} \hat{c}_i \cdot \hat{\mathbf{S}}_i \rangle \propto \langle \hat{s}_i^\dagger \hat{s}_i \rangle$, a non-vanishing vacuum expectation value of \hat{s}_i^\dagger , s , corresponds to the Kondo effect. By virtue of completeness, we have included this approximation in subsection , and the reader will convince oneself that only solutions with a finite value of s will occur, see Fig. S9. As such this approximation invariably predicts *coexistence* of magnetism and the Kondo effect, for *both* the square and honeycomb lattices. This again stands at odds with our QMC results of the main text.

Large- N mean-field approach

The Kondo lattice Hamiltonian given in Eq. (S1) in terms of the fermionic representation of spin operator $\hat{\mathbf{S}}_i = \frac{1}{2} \sum_{\sigma,\sigma'} \hat{f}_{i,\sigma}^\dagger \boldsymbol{\sigma}_{\sigma,\sigma'} \hat{f}_{i,\sigma'}$ with the constraint $\hat{f}_{i,\uparrow}^\dagger \hat{f}_{i,\uparrow} + \hat{f}_{i,\downarrow}^\dagger \hat{f}_{i,\downarrow} = 1$ can be written as,

$$\hat{H} = \sum_{\mathbf{k},\sigma} \epsilon_{\mathbf{k}} \hat{c}_{\mathbf{k},\sigma}^\dagger \hat{c}_{\mathbf{k},\sigma} + \frac{J_k}{4} \sum_i (\hat{f}_{i,\uparrow}^\dagger \hat{f}_{i,\uparrow} - \hat{f}_{i,\downarrow}^\dagger \hat{f}_{i,\downarrow}) (\hat{c}_{i,\uparrow}^\dagger \hat{c}_{i,\uparrow} - \hat{c}_{i,\downarrow}^\dagger \hat{c}_{i,\downarrow}) - \frac{J_k}{4} \sum_i [(\hat{f}_{i,\uparrow}^\dagger \hat{c}_{i,\uparrow} + \hat{c}_{i,\downarrow}^\dagger \hat{f}_{i,\downarrow})^2 + (\hat{f}_{i,\downarrow}^\dagger \hat{c}_{i,\downarrow} + \hat{c}_{i,\uparrow}^\dagger \hat{f}_{i,\uparrow})^2]. \quad (\text{S21})$$

In the large- N approach we allow for Kondo screening as well as antiferromagnetic ordering with the following mean-field decouplings,

$$\langle \hat{f}_{i,\uparrow}^\dagger \hat{f}_{i,\uparrow} - \hat{f}_{i,\downarrow}^\dagger \hat{f}_{i,\downarrow} \rangle = m_f e^{i\mathbf{Q} \cdot \mathbf{i}}, \quad \langle \hat{c}_{i,\uparrow}^\dagger \hat{c}_{i,\uparrow} - \hat{c}_{i,\downarrow}^\dagger \hat{c}_{i,\downarrow} \rangle = -m_c e^{i\mathbf{Q} \cdot \mathbf{i}}, \quad \langle \hat{f}_{i,\uparrow}^\dagger \hat{c}_{i,\uparrow} + \hat{c}_{i,\downarrow}^\dagger \hat{f}_{i,\downarrow} \rangle = \langle \hat{f}_{i,\downarrow}^\dagger \hat{c}_{i,\downarrow} + \hat{c}_{i,\uparrow}^\dagger \hat{f}_{i,\uparrow} \rangle = V. \quad (\text{S22})$$

Here, m_f denotes the staggered magnetization on localized spins, m_c denotes the staggered magnetization of conduction electrons, V denotes the hybridization parameter between \hat{c} and \hat{f} electrons and \mathbf{Q} is the antiferromagnetic ordering wavevector.

For a honeycomb KLM the mean-field Hamiltonian in the momentum space can be written as follows,

$$\hat{H}_{m,f} = \sum_{\mathbf{k},\sigma} \hat{\phi}_{\mathbf{k},\sigma}^\dagger \begin{pmatrix} \frac{J_k m_f \sigma}{4} & Z(\mathbf{k}) & -\frac{J_k V}{2} & 0 \\ Z^\dagger(\mathbf{k}) & -\frac{J_k m_f \sigma}{4} & 0 & -\frac{J_k V}{2} \\ -\frac{J_k V}{2} & 0 & -\frac{J_k m_c \sigma}{4} & 0 \\ 0 & -\frac{J_k V}{2} & 0 & \frac{J_k m_c \sigma}{4} \end{pmatrix} \hat{\phi}_{\mathbf{k},\sigma} + e_0 N_u. \quad (\text{S23})$$

Here, $\hat{\phi}_{\mathbf{k},\sigma}^\dagger = \{\hat{\phi}_{\hat{c}_{\mathbf{k},a},\sigma}^\dagger, \hat{\phi}_{\hat{c}_{\mathbf{k},b},\sigma}^\dagger, \hat{\phi}_{\hat{f}_{\mathbf{k},a},\sigma}^\dagger, \hat{\phi}_{\hat{f}_{\mathbf{k},b},\sigma}^\dagger\}$, $e_0 = (\frac{J_k V^2}{2} + \frac{J_k m_f m_c}{4})$, $Z(\mathbf{k}) = -t(1 + e^{-i\mathbf{k}\cdot\mathbf{a}_2} + e^{-i\mathbf{k}\cdot(\mathbf{a}_2-\mathbf{a}_1)})$ with $\mathbf{a}_1 = (1, 0)$ and $\mathbf{a}_2 = (\frac{1}{2}, \frac{\sqrt{3}}{2})$ and N_u is the number of unit cells.

Diagonalization of the mean-field Hamiltonian gives the following dispersion relations,

$$E_{\mathbf{k},n} = \mp \frac{1}{4} \sqrt{P_{\mathbf{k}} \mp \frac{1}{2} \sqrt{Q_{\mathbf{k}} - 4R_{\mathbf{k}}}} \quad (\text{S24})$$

with,

$$\begin{aligned} P_{\mathbf{k}} &= 8|Z(\mathbf{k})|^2 + (m_c^2 J_k^2)/2 + (m_f^2 J_k^2)/2 + 4J_k^2 V^2, \\ Q_{\mathbf{k}} &= (-16|Z(\mathbf{k})|^2 - m_c^2 J_k^2 - m_f^2 J_k^2 - 8J_k^2 V^2)^2, \\ R_{\mathbf{k}} &= (16m_c^2 |Z(\mathbf{k})|^2 J_k^2 + m_c^2 m_f^2 J_k^4 + 8m_c m_f J_k^4 V^2 + 16J_k^4 V^4). \end{aligned}$$

The ground state energy per unit cell can be computed as,

$$e_g = e_0 + \frac{2}{N_u} \sum_{\mathbf{k},n,E_{\mathbf{k},n}<0} E_{\mathbf{k},n}. \quad (\text{S25})$$

The self consistent equations of mean-field parameters can be obtained from the saddle point approximation,

$$\frac{de_g}{dV} = 0, \quad \frac{de_g}{dm_f} = 0, \quad \frac{de_g}{dm_c} = 0. \quad (\text{S26})$$

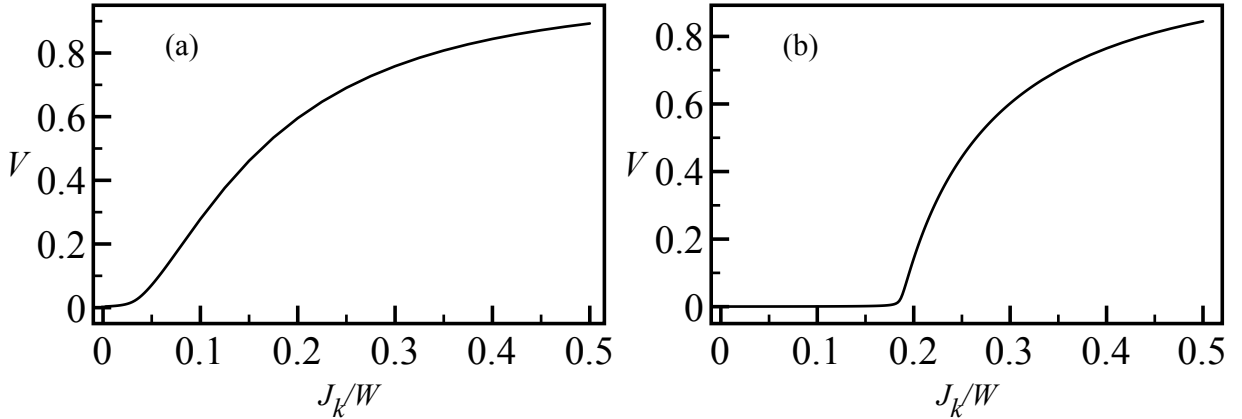


FIG. S7. Hybridization parameter V as a function of J_k/W in the absence of magnetic order computed within the large- N mean-field approach. (a) For a square KLM. (b) For a honeycomb KLM.

Figures S7(a) and S7(b) plot the hybridization order parameter as a function of J_k/W on the square and honeycomb lattices in the absence of magnetic order. Figure S8 was obtained by taking into account both Kondo screening and magnetic order and plots the mean-field order parameters m_f , m_c , and V as a function of J_k/W for the honeycomb KLM.

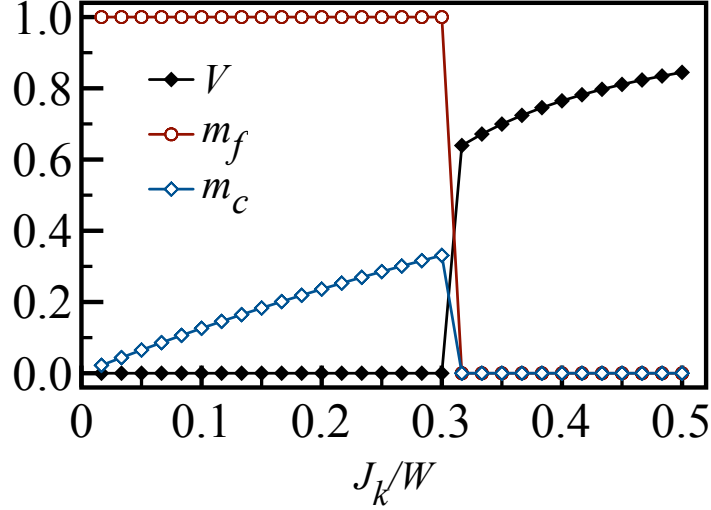


FIG. S8. Mean-field order parameters as a function of J_k/W for the honeycomb KLM within the large- N mean-field approach.

Bond fermion mean-field theory

To formulate the bond fermion mean-field theory we consider the states:

$$\begin{aligned}
\hat{s}_i^\dagger |0\rangle &= \frac{1}{\sqrt{2}} \left(\hat{c}_{i,\uparrow}^\dagger \hat{f}_{i,\downarrow}^\dagger - \hat{c}_{i,\downarrow}^\dagger \hat{f}_{i,\uparrow}^\dagger \right) |0\rangle \\
\hat{t}_{i,0}^\dagger |0\rangle &= \frac{1}{\sqrt{2}} \left(\hat{c}_{i,\uparrow}^\dagger \hat{f}_{i,\downarrow}^\dagger + \hat{c}_{i,\downarrow}^\dagger \hat{f}_{i,\uparrow}^\dagger \right) |0\rangle \\
\hat{t}_{i,\sigma}^\dagger |0\rangle &= \hat{c}_{i,\sigma}^\dagger \hat{f}_{i,\sigma}^\dagger |0\rangle \\
\hat{h}_{i,\sigma}^\dagger |0\rangle &= \hat{f}_{i,\sigma}^\dagger |0\rangle \\
\hat{d}_{i,\sigma}^\dagger |0\rangle &= \hat{c}_{i,\uparrow}^\dagger \hat{c}_{i,\downarrow}^\dagger \hat{f}_{i,\sigma}^\dagger |0\rangle.
\end{aligned} \tag{S27}$$

Here, \hat{s}_i^\dagger and $\hat{t}_{1,0,-1}^\dagger$ denote a singlet and three triplet states with one conduction electron per site and \hat{h}_σ^\dagger and \hat{d}_σ^\dagger denote holons and doublons of the conduction electrons. In this representation, the constraint

$$\hat{s}_i^\dagger \hat{s}_i + \sum_{m=1,0,-1} \hat{t}_{i,m}^\dagger \hat{t}_{i,m} + \sum_{\sigma=\uparrow,\downarrow} (\hat{h}_{i,\sigma}^\dagger \hat{h}_{i,\sigma} + \hat{d}_{i,\sigma}^\dagger \hat{d}_{i,\sigma}) = 1 \tag{S28}$$

suppresses the unphysical states.

The conduction electron operator and the spin operators on \hat{f} and \hat{c} electrons in the above representation take the following forms,

$$\hat{c}_{i,\sigma}^\dagger = \frac{\sigma}{\sqrt{2}} (\hat{s}_i^\dagger + \sigma \hat{t}_{i,0}^\dagger) \hat{h}_{i,-\sigma} + \hat{t}_{i,\sigma}^\dagger \hat{h}_{i,\sigma} - \frac{\hat{d}_{i,\sigma}^\dagger}{\sqrt{2}} (\hat{s}_i - \sigma \hat{t}_{i,0}) + \sigma \hat{d}_{i,-\sigma}^\dagger \hat{t}_{i,-\sigma} \tag{S29}$$

$$\hat{S}_{i,\alpha} = \frac{1}{2} (\hat{s}_i^\dagger \hat{t}_{i,\alpha} + \hat{t}_{i,\alpha}^\dagger \hat{s}_i - i \epsilon_{\alpha\beta\gamma} \hat{t}_{i,\beta}^\dagger \hat{t}_{i,\gamma}) + \hat{S}_{i,\alpha}^h + \hat{S}_{i,\alpha}^d \tag{S30}$$

$$\hat{S}_{i,\alpha}^c = \frac{1}{2} (-\hat{s}_i^\dagger \hat{t}_{i,\alpha} - \hat{t}_{i,\alpha}^\dagger \hat{s}_i - i \epsilon_{\alpha\beta\gamma} \hat{t}_{i,\beta}^\dagger \hat{t}_{i,\gamma}) \tag{S31}$$

where $\epsilon_{\alpha\beta\gamma}$ is the totally antisymmetric tensor, the holon and doublon spin operators read $\hat{S}_{i,\alpha}^h = \frac{1}{2} \sum_{\sigma,\sigma'} \hat{h}_{i,\sigma}^\dagger \boldsymbol{\sigma}_{\sigma,\sigma'} \hat{h}_{i,\sigma'}$ and $\hat{S}_{i,\alpha}^d = \frac{1}{2} \sum_{\sigma,\sigma'} \hat{d}_{i,\sigma}^\dagger \boldsymbol{\sigma}_{\sigma,\sigma'} \hat{d}_{i,\sigma'}$ and the triplon operators are defined as follows,

$$\hat{t}_{i,z}^\dagger |0\rangle = \hat{t}_{i,0}^\dagger |0\rangle, \quad \hat{t}_{i,x}^\dagger |0\rangle = \frac{1}{\sqrt{2}} (\hat{t}_{i,1}^\dagger + \hat{t}_{i,-1}^\dagger) |0\rangle, \quad \hat{t}_{i,y}^\dagger |0\rangle = -\frac{i}{\sqrt{2}} (\hat{t}_{i,1}^\dagger - \hat{t}_{i,-1}^\dagger) |0\rangle. \tag{S32}$$

In the bond fermion mean-field approach to the KLM, the Kondo phase corresponds to condensation of singlets $\langle \hat{s}_i \rangle$ and the SDW phase corresponds to condensation of z component of triplets $\langle \hat{t}_{i,z} \rangle$ in the singlet background. Hence, we consider the following mean-field approximation [60]:

$$\langle \hat{s}_i \rangle = \langle \hat{s}_i^\dagger \rangle = s \quad (\text{S33})$$

$$\langle \hat{t}_{i,z} \rangle = \langle \hat{t}_{i,z}^\dagger \rangle = (-1)^i m \quad (\text{S34})$$

where $(-1)^i = 1(-1)$ on sub-lattice A (B), corresponds to antiferromagnetic ordering.

Using the above approximation the honeycomb Kondo lattice mean-field Hamiltonian can be written as,

$$\begin{aligned} \hat{H}_{mf} = e_0 N_u + \mu \sum_{i,\sigma} \left(\hat{h}_{i,\sigma}^{\dagger a} \hat{h}_{i,\sigma}^a - \hat{d}_{i,\sigma}^a \hat{d}_{i,\sigma}^{\dagger a} + \hat{h}_{i,\sigma}^{\dagger b} \hat{h}_{i,\sigma}^b - \hat{d}_{i,\sigma}^b \hat{d}_{i,\sigma}^{\dagger b} \right) + \frac{1}{2}(s^2 - m^2) \sum_{\langle ij \rangle, \sigma} \left(\hat{h}_{i,\sigma}^{\dagger a} \hat{h}_{j,\sigma}^b + \hat{d}_{i,\sigma}^a \hat{d}_{j,\sigma}^{\dagger b} + \text{H.c.} \right) \\ + \frac{1}{2}(s+m)^2 \sum_{\langle ij \rangle, \sigma} \left(-\hat{h}_{i,-\sigma}^{\dagger a} \hat{d}_{j,\sigma}^{\dagger b} + \hat{d}_{i,-\sigma}^a \hat{h}_{j,\sigma}^b + \text{H.c.} \right) + \frac{1}{2}(s-m)^2 \sum_{\langle ij \rangle, \sigma} \left(\hat{h}_{i,\sigma}^{\dagger a} \hat{d}_{j,-\sigma}^{\dagger b} - \hat{d}_{i,\sigma}^a \hat{h}_{j,\sigma}^b + \text{H.c.} \right). \quad (\text{S35}) \end{aligned}$$

Here, $e_0 = \left(-\frac{3J_k}{4}s^2 + \frac{J_k}{4}m^2 + \mu(s^2 + m^2 + 1) \right)$ and N_u is the number of unit cells. We use the global Lagrange multiplier $\mu_i = \mu$ to impose the constraint $\mu(s^2 + m^2 - 1)$. Note that in the above we have ignored all the terms corresponding to the transverse and longitudinal spin fluctuations.

The mean-field Hamiltonian in momentum space can be written as follows,

$$\hat{H}_{mf} = e_0 N_u + \sum_{\mathbf{k}, \sigma} \phi_{\mathbf{k}, \sigma}^\dagger M(\mathbf{k}) \phi_{\mathbf{k}, \sigma} \quad (\text{S36})$$

where $\phi_{\mathbf{k}, \sigma}^\dagger = \{ \hat{h}_{\mathbf{k}, \sigma}^{\dagger a}, \hat{h}_{\mathbf{k}, \sigma}^{\dagger b}, \hat{d}_{-\mathbf{k}, \sigma}^{\dagger a}, \hat{d}_{-\mathbf{k}, \sigma}^{\dagger b} \}$ and the matrix $M(\mathbf{k})$

$$M(\mathbf{k}) = \begin{pmatrix} \mu & \alpha_{\mathbf{k}} & 0 & 0 & 0 & 0 & 0 & \beta_{\mathbf{k}} \\ \alpha_{\mathbf{k}}^\dagger & \mu & 0 & 0 & 0 & 0 & \gamma_{\mathbf{k}}^\dagger & 0 \\ 0 & 0 & \mu & \alpha_{\mathbf{k}} & 0 & -\gamma_{\mathbf{k}} & 0 & 0 \\ 0 & 0 & \alpha_{\mathbf{k}}^\dagger & \mu & -\beta_{\mathbf{k}}^\dagger & 0 & 0 & 0 \\ 0 & 0 & 0 & -\beta_{\mathbf{k}} & -\mu & \alpha_{\mathbf{k}}^\dagger & 0 & 0 \\ 0 & 0 & -\gamma_{\mathbf{k}}^\dagger & 0 & \alpha_{\mathbf{k}} & -\mu & 0 & 0 \\ 0 & \gamma_{\mathbf{k}} & 0 & 0 & 0 & 0 & -\mu & \alpha_{\mathbf{k}}^\dagger \\ \beta_{\mathbf{k}}^\dagger & 0 & 0 & 0 & 0 & 0 & \alpha_{\mathbf{k}} & -\mu \end{pmatrix}$$

with

$$\alpha_{\mathbf{k}} = -\frac{1}{2}(s^2 - m^2)Z(\mathbf{k}), \quad \beta_{\mathbf{k}} = -\frac{1}{2}(s+m)^2Z(\mathbf{k}), \quad \gamma_{\mathbf{k}} = -\frac{1}{2}(s-m)^2Z(\mathbf{k}), \quad Z(\mathbf{k}) = -t(1 + e^{-i\mathbf{k} \cdot \mathbf{a}_2} + e^{-i\mathbf{k} \cdot (\mathbf{a}_2 - \mathbf{a}_1)}).$$

The matrix $M(\mathbf{k})$ can be diagonalized via unitary transformation which gives the following dispersion relations for z component of spin $\sigma = \uparrow (\downarrow)$,

$$E_{\mathbf{k}, n} = \mp \sqrt{\frac{1}{2}(m^2 + s^2)^2 |Z(\mathbf{k})|^2 + \mu^2 \mp 2\sqrt{\frac{1}{4}\mu^2 |Z(\mathbf{k})|^2 (m^2 - s^2)^2 + \frac{1}{16}|Z(\mathbf{k})|^4 (m^2 + s^2)^4}}. \quad (\text{S37})$$

The mean-field ground state energy per unit cell can be computed as follows,

$$e_g = e_0 + \frac{2}{N_u} \sum_{\mathbf{k}, n, E_{\mathbf{k}, n} < 0} E_{\mathbf{k}, n}. \quad (\text{S38})$$

Next, using the saddle point approximation,

$$\frac{de_g}{ds} = 0, \quad \frac{de_g}{d\mu} = 0, \quad \frac{de_g}{dm} = 0 \quad (\text{S39})$$

we obtain the following self consistent equations for mean-field parameters μ , m^2 , and s^2 ,

$$\mu = \frac{J_k}{4} - \frac{1}{2N_u} \sum_{\mathbf{k}} |Z(\mathbf{k})|^2 (m^2 + s^2) \left(\frac{1}{E_{\mathbf{k},1}} + \frac{1}{E_{\mathbf{k},2}} \right) - \frac{1}{4N_u} \sum_{\mathbf{k}} \frac{|Z(\mathbf{k})|^4 (m^2 + s^2)^3}{2A_{\mathbf{k}}} \left(\frac{1}{E_{\mathbf{k},1}} - \frac{1}{E_{\mathbf{k},2}} \right) \quad (\text{S40})$$

$$m^2 = \frac{1}{2N_u} \sum_{\mathbf{k}} \frac{|Z(\mathbf{k})|^2 \mu^2 m^2 (s^2 - m^2)}{J_k A_{\mathbf{k}}} \left(\frac{1}{E_{\mathbf{k},1}} - \frac{1}{E_{\mathbf{k},2}} \right) \quad (\text{S41})$$

$$s^2 = -1 - m^2 - \frac{1}{N_u} \sum_{\mathbf{k}} \mu \left(\frac{1}{E_{\mathbf{k},1}} + \frac{1}{E_{\mathbf{k},2}} \right) - \frac{1}{N_u} \sum_{\mathbf{k}} \frac{|Z(\mathbf{k})|^2 (s^2 - m^2)^2 \mu}{4A_{\mathbf{k}}} \left(\frac{1}{E_{\mathbf{k},1}} - \frac{1}{E_{\mathbf{k},2}} \right) \quad (\text{S42})$$

where $E_{\mathbf{k},1}$ and $E_{\mathbf{k},2}$ are the two lowest quasiparticle bands and $A_{\mathbf{k}}$ has the following form,

$$A_{\mathbf{k}} = \sqrt{\frac{1}{4} \mu^2 |Z(\mathbf{k})|^2 (m^2 - s^2)^2 + \frac{1}{16} |Z(\mathbf{k})|^4 (m^2 + s^2)^4}.$$

The magnetization of c and f electrons can be computed as follows,

$$m_c = \frac{2}{N_u} \sum_i (-1)^i \langle \hat{S}_{z,i}^c \rangle = 2ms \quad (\text{S43})$$

$$m_f = \frac{2}{N_u} \sum_i (-1)^i \langle \hat{S}_{z,i} \rangle = 2ms + \frac{1}{N_u} \sum_{\mathbf{k}} \frac{2|Z(\mathbf{k})|^2 \mu ms (s^2 + m^2)}{E_{1,\mathbf{k}} E_{2,\mathbf{k}} (E_{1,\mathbf{k}} + E_{2,\mathbf{k}})}. \quad (\text{S44})$$

Figure S9 plots the mean-field order parameters obtained within the bond fermion mean-field approach as a function of J_k/W for the honeycomb KLM.

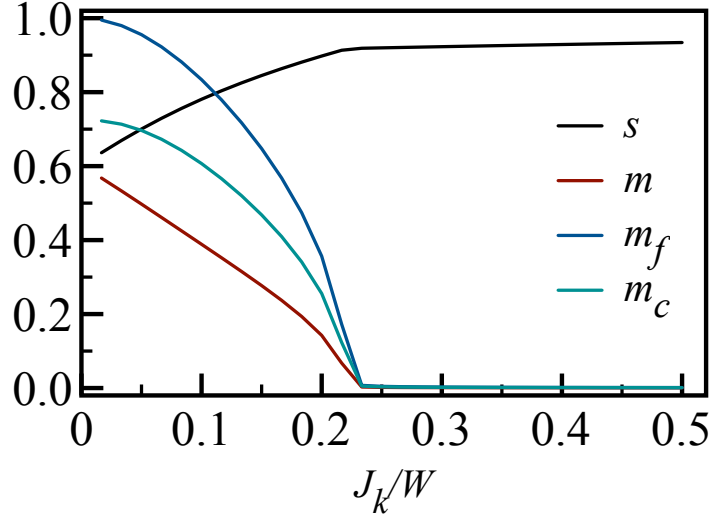


FIG. S9. Mean-field order parameters as a function of J_k/W for the honeycomb KLM within the bond fermion mean-field approach.